Brilacidin, a COVID-19 Drug Candidate, demonstrates broad-spectrum antiviral activity against human coronaviruses OC43, 229E and NL63 through targeting both the virus and the host cell

Yanmei Hu[1], Hyunil Jo[2], William F. DeGrado[2], and Jun Wang[1]*

[1]Department of Pharmacology and Toxicology, College of Pharmacy, The University of Arizona, Tucson, Arizona 85721, United States

[2]Department of Pharmaceutical Chemistry, School of Pharmacy, University of California, San Francisco, California 94158, United States

*Corresponding author:

Jun Wang, Tel: 520-626-1366, Fax: 520-626-0749, email: junwang@pharmacy.arizona.edu

Abstract

Brilacidin, a mimetic of host defense peptides (HDPs), is currently in phase 2 clinical trial as an antibiotic drug candidate. A recent study reported that brilacidin has antiviral activity against SARS-CoV-2 by inactivating the virus. In this work, we discovered an additional mechanism of action of brilacidin by targeting heparan sulfate proteoglycans (HSPGs) on host cell surface. Brilacidin, but not acetyl brilacidin, inhibits the entry of SARS-CoV-2 pseudovirus into multiple cell lines, and heparin, a HSPG mimetic, abolishes the inhibitory activity of brilacidin on SARS-CoV-2 pseudovirus cell entry. In addition, we found that brilacidin has broad-spectrum antiviral activity against multiple human coronaviruses (HCoVs) including HCoV-229E, HCoV-OC43, and HCoV-NL63. Mechanistic studies revealed that brilacidin has a dual antiviral mechanism of action including virucidal activity and binding to coronavirus attachment factor HSPGs on host cell surface. Brilacidin partially loses its antiviral activity when heparin was included in the cell cultures, supporting the host-targeting mechanism. Drug combination therapy showed that brilacidin has a strong synergistic effect with remdesivir against HCoV-OC43 in cell culture. Taken together, this study provides appealing findings for the translational potential of brilacidin as a broad-spectrum antiviral for coronaviruses including SARS-CoV-2.

Keywords: SARS-CoV-2, brilacidin, COVID19, human coronavirus, HSPGs, antiviral.

INTRODUCTION

Seven coronaviruses are known to infect human beings. Human coronavirus (HCoV)-229E, -NL63, -OC43 and -HKU1 account for 15~30% cases of common cold worldwide [1], while severe acute respiratory syndrome coronavirus (SARS-CoV) [2], Middle East Respiratory Syndrome (MERS-CoV) [3], and severe acute respiratory syndrome coronavirus 2 (SARS-CoV-2)-the causative agent of COVID-19 [4], are three highly pathogenic human coronaviruses that cause acute severe respiratory syndrome. As the third coronavirus that causes severe respiratory disease, SARS-CoV-2 associated COVID19 has led to more than 211 million infections and over 4.4 million deaths worldwide, and more than 37 million infections and over 627 thousand deaths in the U.S. alone as of Aug 21, 2021 [5]. Currently, two mRNA vaccines are authorized for COVID-19: BNT162b2 (Pfizer, Inc., and BioNTech) and mRNA-1273 (ModernaTX, Inc.), and a third single-dose COVID-19 vaccine JNJ-78436735 (Johnson & Johnson) was issued for Emergency Use Authorization. Although vaccine continues to be a mainstay for viral prophylaxis, the efficacy of vaccine might be compromised with emerging variants such as the delta variant [6-8]. For this reason, small molecular antiviral drugs are important complements of vaccines to help combat pandemics.

Host defense peptides (HDPs), also called antimicrobial peptides (AMPs), are typically small peptides (12-50 amino acids) that are expressed in neutrophils and mucosa and serve as the first line of defense against foreign pathogens [9]. HDPs have been extensively explored as antibiotics [10], antivirals [11], antifungals [12] and anticancer agents [13]. Most HDPs share an amphiphilic structure with a positively charged face and a hydrophobic face [14]. It is proposed that HDPs disrupt bacterial cell membranes by

interacting with the negatively charged phospholipid headgroups [15-17]. Brilacidin is a small synthetic HDP mimetic [18], and has potent antibacterial activity against both Gram-positive and Gram-negative bacteria, and is currently in Phase 2 clinical trials (Clinical Trials NCT01211470, NCT020388, and NCT02324335). The antibacterial mechanisms of action of brilacidin include both membrane disruption and immunomodulation [19, 20]. Brilacidin is also in clinical trial (NCT04784897) as a SARS-CoV-2 antiviral drug candidate for hospitalized COVID-19 patients. A recent study showed that brilacidin exhibited potent inhibitory effect on SARS-CoV-2 replication (EC_{50}=0.565 μM/CC_{50}=241 μM), and the proposed mechanism of action is through disrupting viral integrity, thereby blocking viral entry [21]. However, the effect of brilacidin on host cell and the antiviral activity of brilacidin against other HCoVs have not been investigated.

In this work, we showed that brilacidin inhibits SARS-CoV-2 pseudovirus entry into multiple cell lines. However, acetyl brilacidin had no inhibition on SARS-CoV-2 pseudovirus entry, and heparin, a heparan sulfate proteoglycans (HSPGs) mimetic, diminished the inhibitory activity of brilacidin. This result suggests that brilacidin has an additional mechanism of action by binding to HSPGs on the host cell, thereby blocking viral attachment. HSPGs have been reported as an attachment factor for SARS-CoV-2 [22, 23]. In addition, we have shown that brilacidin has broad-spectrum antiviral activity against multiple HCoVs including HCoV-229E, HCoV-OC43, and HCoV-NL63. The antiviral mechanism against these viruses similarly involves both virucidal effects and binding to HSPGs. Brilacidin partially loses its antiviral activity against HCoV-229E, HCoV-OC43, HCoV-NL63 in the presence of heparin in cell culture. Drug time-of-addition experiments provided additional evidence that brilacidin exerts its antiviral

activity at both viral attachment and early entry stage of viral life cycle. Finally, drug combination therapy demonstrated that brilacidin has strong synergistic effect with remdesivir against HCoV-OC43 in cell culture. Overall, brilacidin appears to have appealing translational potential as a broad-spectrum antiviral for coronaviruses including SARS-CoV-2.

RESULTS AND DISCUSSION

Brilacidin inhibits SARS-CoV-2 pseudovirus entry in multiple cell lines

To delineate whether brilacidin blocks SARS-CoV-2 viral entry, we generated pseudotyped HIV-1-derived lentiviral particles with SARS-CoV-2 spike protein [24], which is widely used to study spike-mediated viral entry into host cells in biosafety level 2 facilities [25, 26]. Brilacidin was tested in SARS-CoV-2 pseudovirus entry assay in several ACE2-expressing cell lines including Vero C1008, Calu-3, Huh-7, Caco-2, and 293T-ACE2. Vero C1008 and 293T-ACE2 express minimal levels of transmembrane serine proteinase 2 (TMPRSS2), therefore SARS-CoV-2 virus enters into these cell lines mainly through endocytosis and relies on endosomal cathepsin L for viral spike protein activation [27, 28]. In contrast, Calu-3 and Caco-2 endogenously express TMPRSS2 [29], which activates SARS-CoV-2 spike protein on cell surface so virus gets into these cell lines through direct cell membrane fusion. Cathepsin L inhibitor E-64d and TMPRSS2 inhibitor camostat mesylate were included as controls [30]. Our results showed that brilacidin inhibited SARS-CoV-2 pseudovirus entry into all cell lines tested with IC_{50} values ranging from 12.0 ± 1.7 to 23.0 ± 1.6 μM (**Figure 1**). Cytotoxicity assays

showed that brilacidin was not toxic to all the cell lines tested at the concentrations examined (**Figure 1F**). Overall, brilacidin inhibits SARS-CoV-2 pseudovirus entry into multiple cell lines. These results suggest the antiviral activity of brilacidin is independent of cathepsin L or TMPRSS2 inhibition.

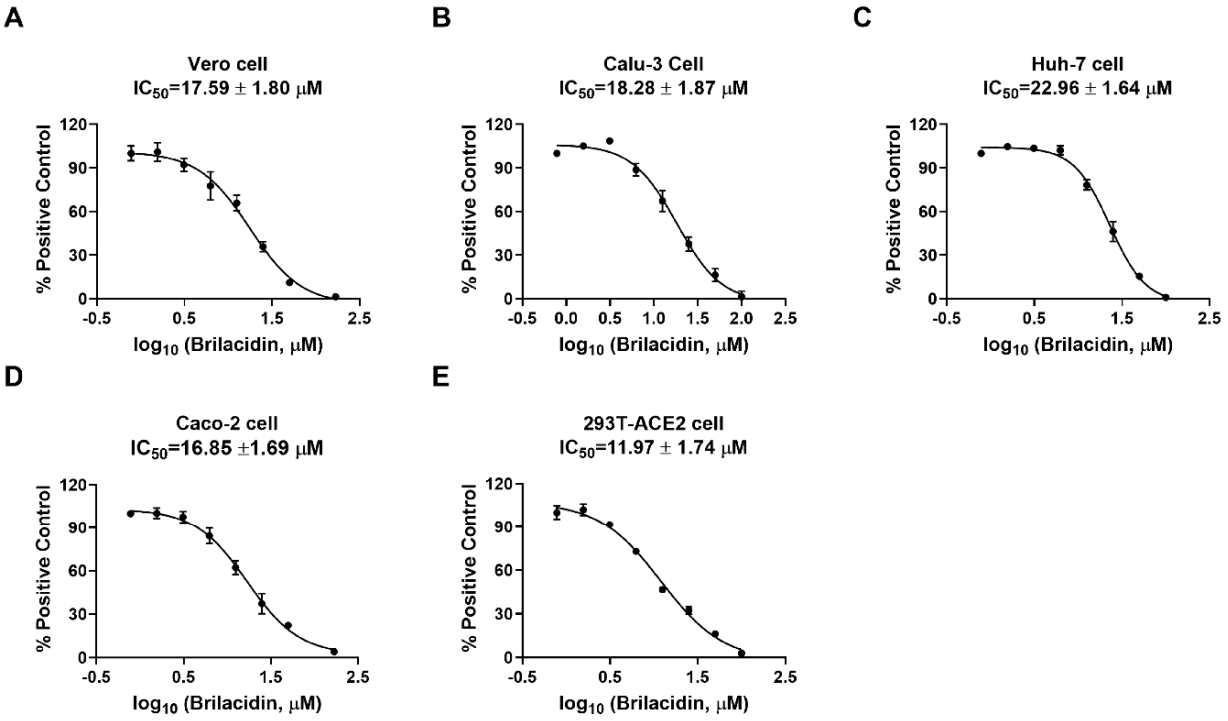

F

Cell lines	brilacidin		Camostat mesylate (IC_{50} μM)[a]	E-64d (IC_{50} μM)[a]
	IC_{50} (μM)	CC_{50} (μM)		
Vero	17.59 ± 1.80	79.48 ± 2.42	>50	0.91 ± 0.097
Calu-3	18.28 ± 1.87	>125	0.16 ± 0.028	>50
Caco-2	16.85 ± 1.69	>125		
Huh-7	22.96 ± 1.64	>125		
293T-ACE2	11.97 ± 1.94	>125		

Figure 1. Inhibition of brilacidin on SARS-CoV-2 pseudovirus entry into multiple cell lines including (A) Vero C1008 cells; (B) Calu-3 cells; (C) Huh-7 cells; (D) Caco-2 cells; (E) 293T-ACE2 cells. (F) Cytotoxicity (CC_{50}) and inhibitory activity (IC_{50}) of brilacidin in SARS-CoV-2 pseudovirus entry assay in different cell lines. [a]Data from ref [31]. IC_{50} and

CC_{50} values were determined through curve fitting described in the "material and methods" section, and all data are mean ± standard deviation of three replicates.

Brilacidin has broad-spectrum antiviral activity against multiple human coronaviruses, but not influenza or enterovirus

It was recently reported that brilacidin exhibited potent antiviral activity on SARS-CoV-2 replication in both Vero and Calu-3 cells [21]. To test whether brilacidin inhibits the replication of other human coronaviruses, we first tested the antiviral activity of brilacidin against HCoV-229E, HCoV-OC43 and HCoV-NL63 in a viral yield reduction (VYR) assay. The results showed that brilacidin inhibited the replication of HCoV-NL63, HCoV-OC43 and HCoV-229E with EC_{50} values of 2.45 ± 0.05 μM, 4.81 ± 0.95 μM, 1.59 ± 0.07 μM, respectively (**Figure 2A, 2B, 2C**). To confirm the antiviral activity of brilacidin, we tested its inhibitory effect on viral replication over different time course up to 5 days post infection (dpi). HCoV-229E, HCoV-NL63, and HCoV-OC43 were propagated in the presence or absence of brilacidin, and the cell culture supernatants were collected at different time points post infection. Viral titer from each sample was determined by plaque assay. The results demonstrated that brilacidin decreased the viral tiers of all three human coronaviruses by at least 1 log_{10} unit at all time points (**Figure 2D, 2E, 2F**). Brilacidin also inhibited HCoV-OC43 in the plaque assay with an EC_{50} of 7.32 ± 0.15 μM (**Figure 2G, top panel**). In contrast, brilacidin had no effect on the replication of either the influenza A/California/07/2009 (H1N1) virus (**Figure 2G, middle panel**) or enterovirus D68 US/MO/14-18947 (**Figure 2G, bottom panel**) in the plaque assay. The selectivity indices (SI) of brilacidin, which were calculated as the ratio of CC_{50} over EC_{50},

range from 17.1 to greater than 64.1 for HCoV-OC43, HCoV-NL63, and HCoV-229E, respectively (**Figure 2H**). Taken together, these results indicate that brilacidin has potent antiviral activity against human coronaviruses, but not influenza or enterovirus D68.

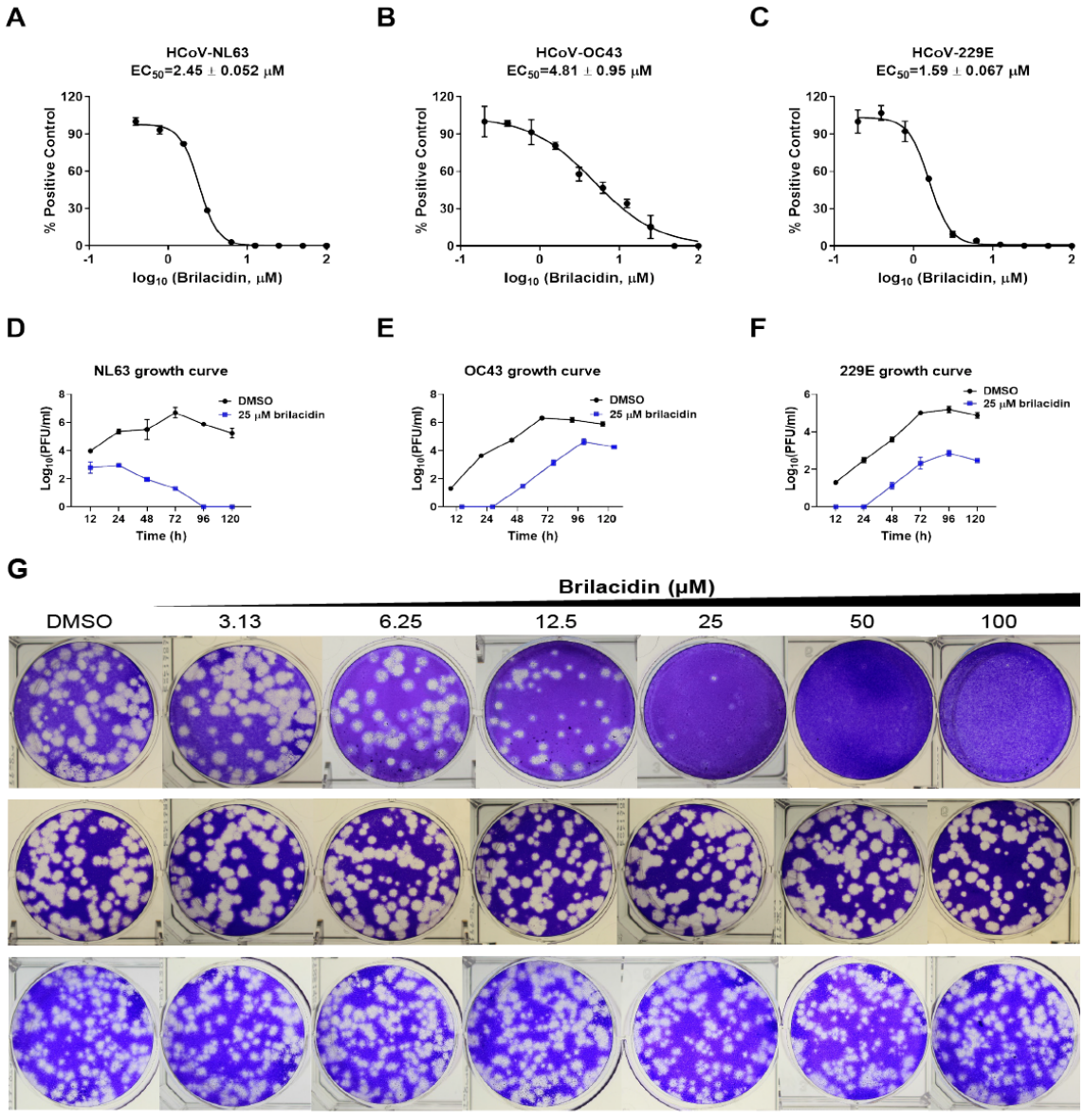

H

Coronaviruses	Cell line	EC_{50} (μM)	CC_{50} (μM)	SI
HCoV-OC43	RD cell	4.81 ± 0.95 (VYR)	>125	>26.0
		7.32 ± 0.15 (plaque)		>17.1
HCoV-229E	Huh-7 cell	1.95 ± 0.067	>125	>64.1
HCoV-NL63	Vero cell	2.45 ± 0.052	79.48 ± 2.42	>32.4

Figure 2. Antiviral activity of brilacidin against multiple human coronaviruses, influenza and enterovirus. Antiviral activity of brilacidin in viral yield reduction assay against HCoV-NL63 (A), HCoV-OC43 (B), and HCoV-229E (C). Growth curve of HCoV-NL63 (D), HCoV-OC43 (E), and HCoV-229E (F) in the presence of DMSO or 25 μM brilacidin. (G) Antiviral activity of brilacidin against HCoV-OC43 (top panel), influenza A/California/07/2009 (H1N1) (middle panel), and enterovirus D68 MO-18947 (bottom panel) in plaque assay. (H) EC_{50} of brilacidin against HCoV-NL63, HCoV-OC43, HCoV-229E; CC_{50} of brilacidin in RD cell, Huh-7 cell, Vero cell; and corresponding SI values. EC_{50} and CC_{50} values were determined through curve fitting described in the "material and methods" section, and all data are mean ± standard deviation of three replicates.

Brilacidin targets both the virus and the host cell

To elucidate the antiviral mechanism of brilacidin, we first performed experiments to determine whether brilacidin directly targets the virus or the host cell. To assess the virucidal effect of brilacidin on human coronaviruses, we incubated HCoV-OC43, HCoV-229E or HCoV-NL63 with serial concentrations of brilacidin (25, 50, 100, 200 μM) or DMSO at 37 °C for 14 hrs. The mixture was then diluted 10^6-fold to quantify the infectious viral titer. The final concentrations of brilacidin in each sample after dilution were 0.025, 0.05, 0.1 and 0.2 nM, respectively, which are far below its minimum inhibitory concentration (EC_{50}s in the low μM range) and therefore had no effect on plaque formation. It was found that brilacidin treatment decreased the viral titers of all three human coronaviruses dose-dependently, and the viral titers were decreased by more than 1 $\log_{10}$ unit at 200 μM (**Figure 3A, 3B, 3C**), meaning over 90% of the viral

particles were inactivated by brilacidin treatment. To evaluate the effect of brilacidin on host cells, Huh-7, Vero C1008, and RD cells were pre-treated with serial concentrations of brilacidin (25, 50, 100 μM) or DMSO at 37 °C for 14 hrs, and the cells were subsequently washed with PBS buffer supplemented with magnesium and calcium three times to remove brilacidin. Then the pre-treated cells were infected with HCoV-229E, HCoV-NL63 and HCoV-OC43 at a MOI of 0.1 in the absence of brilacidin. Cell culture supernatants were collected 24 hpi and the viral titers were determined by plaque assay (**Figure 3D, 3E, 3F**). The results demonstrated that pre-treatment of host cells with brilacidin dose-dependently inhibited virus replication and this inhibitory effect is not cell type dependent. Taken together, these results suggest that the antiviral effect of brilacidin involves targeting both the virus and the host cell.

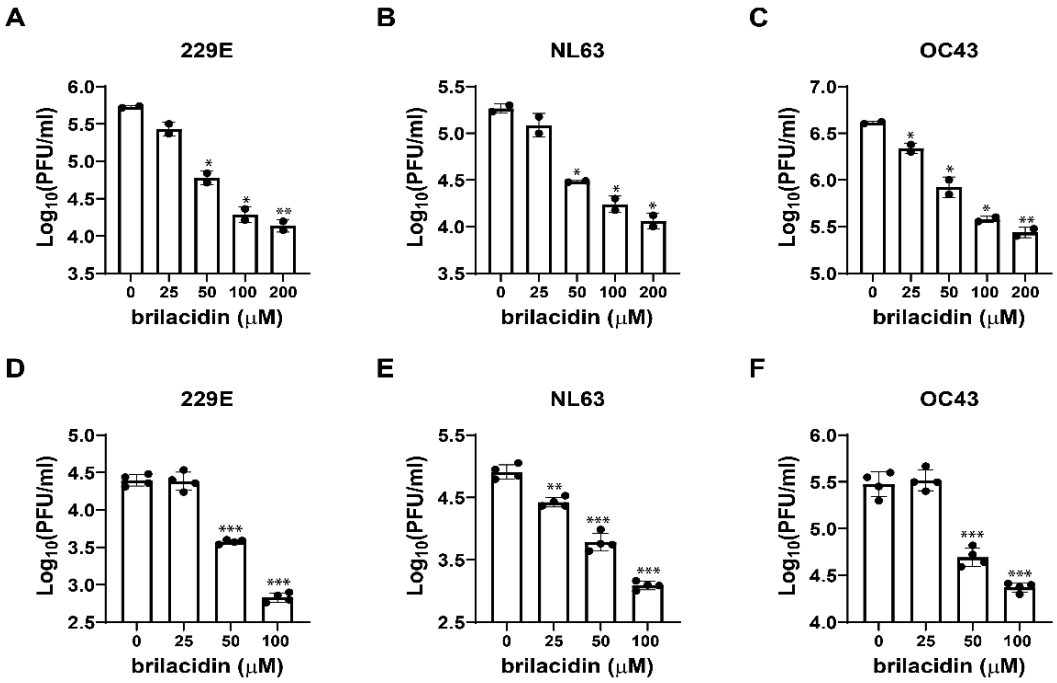

Figure 3. Effect of brilacidin on human coronavirus particles and host cells. Virucidal effect of brilacidin on HCoV-229E (A), HCoV-NL63 (B), and HCoV-OC43 (C). Effects of

pre-treatment of cells with brilacidin on the viral replication of HCoV-229E (D), HCoV-NL63 (E), and HCoV-OC43 (F). HCoV-229E, HCoV-NL63, and HCoV-OC43 were propagated in Huh-7, Vero C1008, and RD cells, respectively. *, $p < 0.05$; **, $p < 0.01$; ***, $p < 0.001$ (student's *t*-test). Data in (A), (B) and (C) are mean ± standard deviation of duplicates, and Data in (D), (E) and (F) are mean ± standard deviation of quadruplicates.

Brilacidin blocks virus attachment and early entry into host cells

Next, drug time-of-addition experiment was carried out to determine at which step(s) of viral life cycle brilacidin exerts its antiviral activity. In this experiment, 50 µM of brilacidin was added into the cell culture at different time points of viral replication as illustrated in **Figure 4B**. Brilacidin was included in viral attachment and onwards (#1: -2→14h), viral attachment and entry (#2: -2→0h), viral attachment only (#3: -2→-1h), viral entry and onwards (#4: -1→14h), viral entry only (#5: -1→0h), and different time points post-viral entry (#6-#11). To detect intracellular viral protein levels, RD cells were infected with HCoV-OC43 at an MOI of 1 and cells were fixed 14 hpi for immunofluorescence staining using HCoV-OC43 specific N protein antibody. The immunofluorescence signal was significantly decreased at two time points when brilacidin was added during viral attachment (#1, #2, #3) and the early entry stage (#4, #6, #7) (**Figure 4A**). To quantify progeny viruses released into the cell culture medium, RD cells and Huh-7 cells were infected with HCoV-OC43 and HCoV-229E at an MOI of 0.1, respectively. Viruses in the cell culture medium were collected and the viral titers were determined by plaque assay. Consistent with the immunofluorescence staining

results, both HCoV-OC43 and HCoV-229E viral titers decreased considerably when brilacidin was added during the viral attachment (#1, #2, #3) and the early entry stage (#4, #6, #7) (**Figure 4C, 4D**). As shown by the results from both intracellular viral protein level detected by immunofluorescence staining and virus released into cell culture medium quantified by plaque assay, brilacidin exerted the greatest inhibitory effect when it was present at all time points (#1). In conclusion, the drug time-of-addition experiment suggested that brilacidin blocks both viral attachment and early entry into host cells, supporting that it has a dual antiviral mechanism of action.

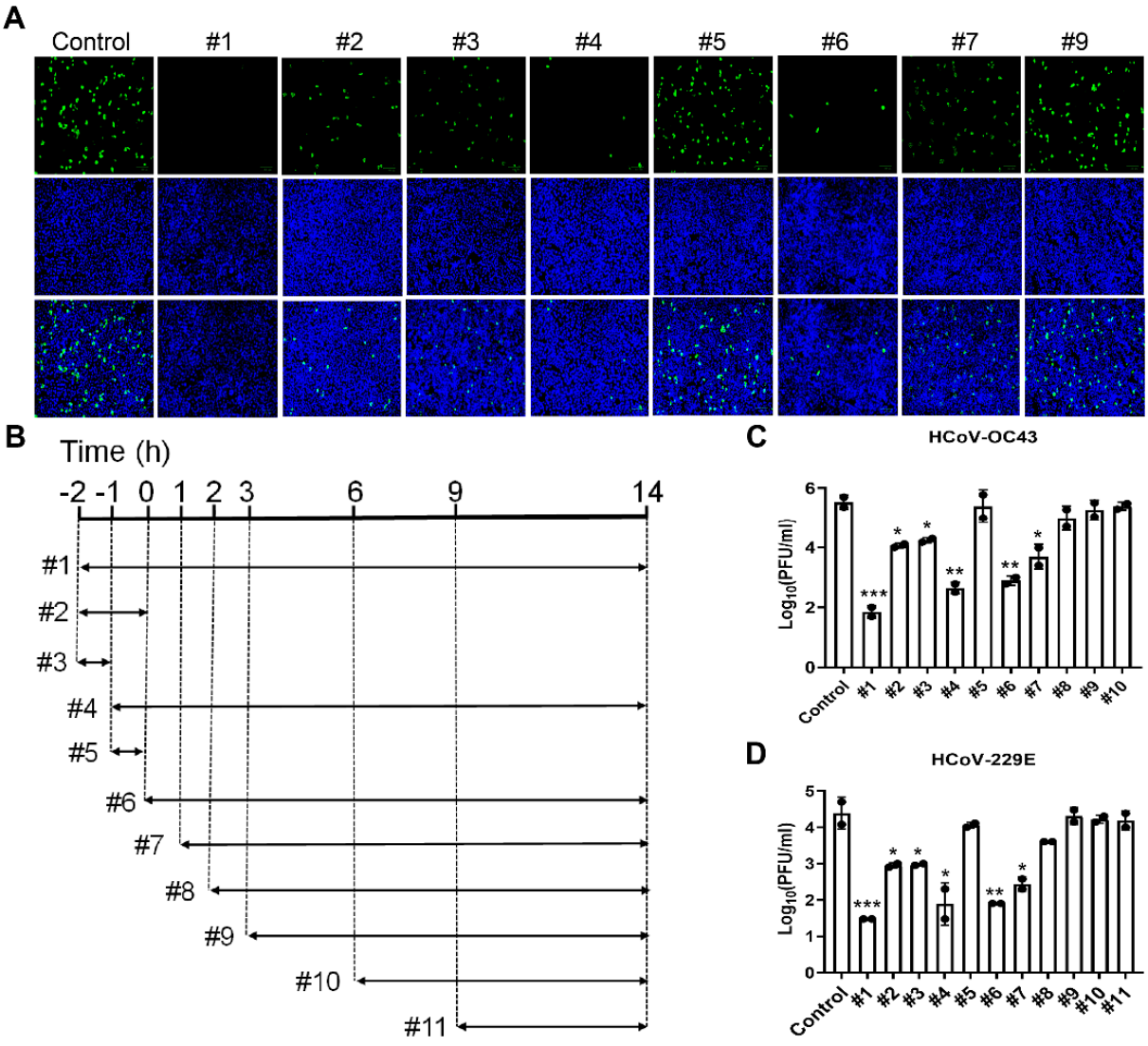

Figure 4. Time-of-addition experiments of brilacidin in inhibiting HCoV-OC43 and HCoV-229E. (A) Representative images of intracellular HCoV-OC43 viral protein detected by immunofluorescence staining using HCoV-OC43 specific antibody. Images were taken by Zoe™ Fluorescent Cell Imager (BioRad); (B) Illustration of the time periods when 50 μM brilacidin was present in the time-of-addition experiments. Arrows represent the periods of time that brilacidin was present in the cell culture; Quantification of HCoV-OC43 (C) or HCoV-229E (D) virus released into the cell culture medium using plaque assay. *, $p < 0.05$; **, $p < 0.01$, ***, $p < 0.001$ (student's *t*-test). Data are mean ± standard deviation of duplicates.

Heparin decreases the inhibitory activity of brilacidin in SARS-CoV-2 pseudovirus cell entry and HCoV-OC43, HCoV-229E and HCoV-NL63 replication in cell culture

It was proposed that brilacidin binds to SARS-CoV-2 spike protein [30]. To test whether brilacidin blocks SARS-CoV-2 pseudovirus entry into host cells through interaction with the spike protein, we tested the direct binding of brilacidin to SARS-CoV-2 spike protein receptor binding domain (RBD) using differential scanning fluorimetry (DSF). The results demonstrated that brilacidin has no effect on the melting temperature (T_m) of SARS-CoV-2 spike protein RBD up to 100 μM (**Table 1**), indicating that there is no direct binding between brilacidin and SARS-CoV-2 spike protein RBD.

Table 1. Effect of brilacidin on melting temperature (T_m) of SARS-CoV-2 spike RBD.

Compound	**T_m (°C)**	**ΔT_m (°C)**
DMSO	48.05	
25 μM brilacidin	47.96	-0.09
50 μM brilacidin	48.23	0.18
100 μM brilacidin	48.02	-0.03

HSPGs are negatively charged, linear polysaccharide that are abundantly expressed on the surface of almost all types of mammalian cells [32]. It has been reported that HCoV-NL63 utilizes cell surface HSPGs as adhesion receptor for viral attachment to target cells through its interaction with the membrane (M) protein [33, 34]. Also, cell surface HSPGs were discovered as the attachment factors for SARS-CoV-2 and facilitate the subsequent binding of spike protein to ACE2 receptor [35-37]. Brilacidin is +4 charged at neutral pH, we therefore hypothesize that brilacidin might bind to the cell surface HSPGs through electrostatic interactions, thereby blocking viral attachment and entry. To test this hypothesis, we chose acetyl brilacidin, which is +2 charged, as a control compound (**Figure 5A**). It was found that acetyl brilacidin completely lost inhibitory activity in SARS-CoV-2 pseudovirus entry assay in Vero C1008, Calu-3 and Caco-2 cells (**Figure 5B, 5C, 5D**). This result suggests that the +4 charge on brilacidin is critical for the antiviral activity, and the antiviral mechanism of action might involve interaction with the binding to HSPGs.

If brilacidin binds to cell surface HSPGs in cell culture, exogenous addition of HSPG mimetics such as heparin will compete with HSPGs for binding of brilacidin, resulting in

decreased inhibitory activity of brilacidin on SARS-CoV-2 pseudovirus entry and the replication of human coronaviruses in cell culture. We therefore performed the competition assay to evaluate the effect of heparin on the antiviral activity of brilacidin. To test the effect of heparin on brilacidin activity in SARS-CoV-2 pseudovirus entry, heparin was first tested in SARS-CoV-2 pseudovirus entry assay in Vero C1008, Caco-2 and Calu-3 cells to determine proper concentrations in the competition assay. The highest concentration of heparin used in the competition assay was 100 µg/ml, which had no effect on SARS-CoV-2 pseudovirus entry (**Figure 5E**). As expected, addition of heparin dose-dependently abolished the inhibitory activity of brilacidin on SARS-CoV-2 pseudovirus entry into Vero C1008 cells (**Figure 5F**), Calu-3 cells (**Figure 5G**), and Caco-2 cells (**Figure 5H**) as shown by the increasing IC_{50} values. Specifically, heparin increased the IC_{50} values of brilacidin by more than 2-fold and 3 to 5-fold at 10 and 30 µg/ml, respectively (**Figure 5I**). Heparin almost completely abolished the inhibitory activity of brilacidin when added at 100 µg/ml concentration (IC_{50} > 125 µM) (**Figure 5E, 5F, 5G, 5H**).

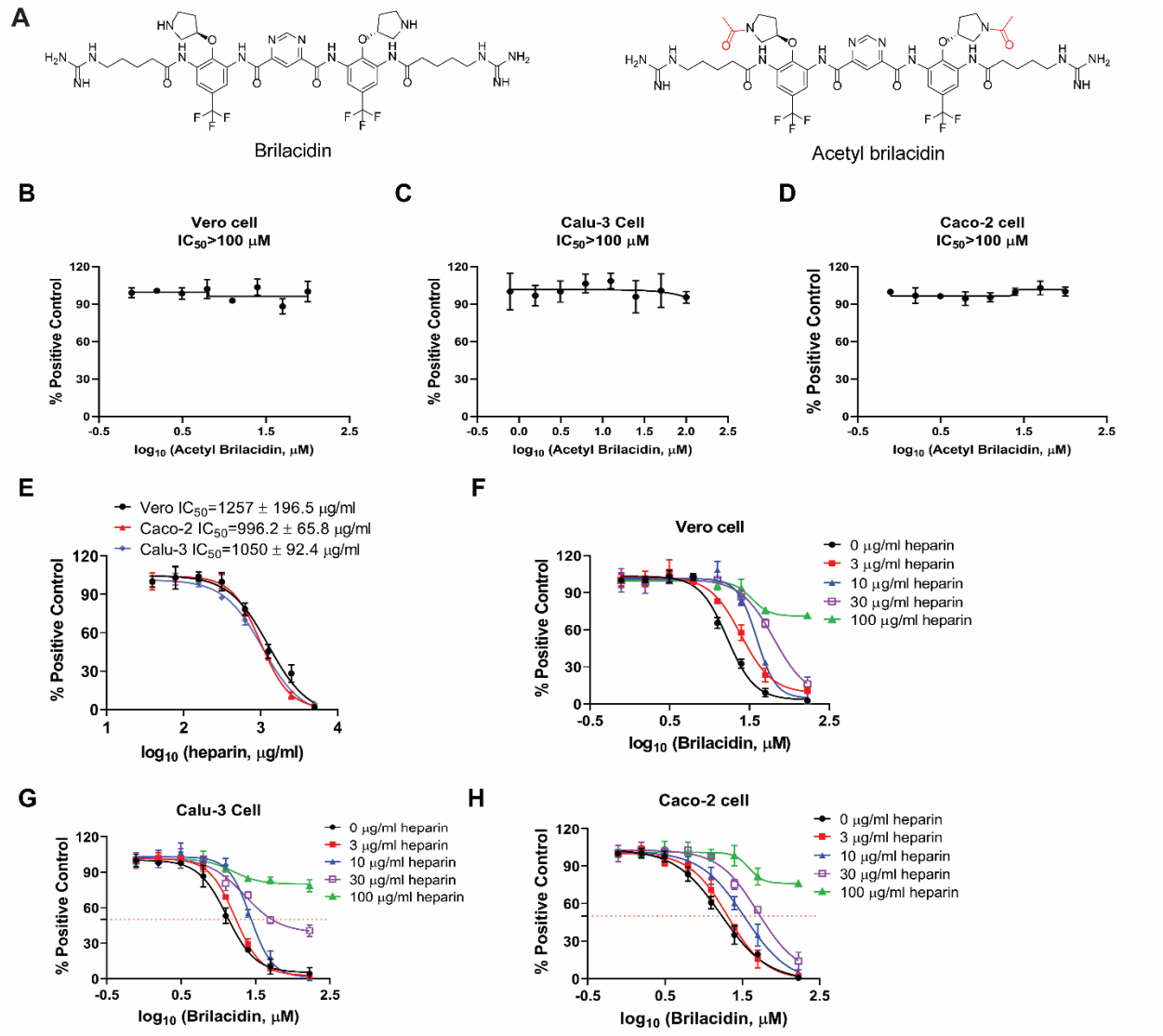

I

Cell lines	brilacidin (IC_{50}, μM)				
	0 μg/ml heparin	3 μg/ml heparin	10 μg/ml heparin	30 μg/ml heparin	100 μg/ml heparin
Vero E6	16.60 ± 1.22	24.83 ± 2.27	38.96 ± 2.47	63.66 ± 12.96	>125
Calu-3	13.06 ± 0.96	16.68 ± 0.59	26.89 ± 1.78	62.97 ± 14.45	>125
Caco-2	16.85 ± 1.69	20.50 ± 1.73	33.92 ± 4.49	50.41 ± 14.34	>125

Figure 5. Heparin diminishes the inhibitory activity of brilacidin in SARS-CoV-2 pseudovirus entry into different cell lines. (A) Chemical structures of brilacidin and acetyl brilacidin. Effect of acetyl brilacidin on SARS-CoV-2 pseudovirus entry into Vero C1008 (B), Calu-3 (C), and Caco-2 (D). (E) IC_{50}s of heparin in SARS-CoV-2 pseudovirus entry assay in Vero C1008 cells, Caco-2 cells and Calu-3 cells. Heparin dose-dependently

decreased the potency of brilacidin in inhibiting SARS-CoV-2 pseudovirus entry into Vero C1008 cells (F), Calu-3 cells (G), and Caco-2 cells (H). (I) Summary of IC_{50}s of brilacidin in SARS-CoV-2 pseudovirus entry assay in the heparin competition assay. IC_{50} values were determined through curve fitting described in the "material and methods" section, and all data are mean ± SD of two independent experiments.

To test whether heparin affects the inhibition of human coronaviruses by brilacidin, HCoV-229E, HCoV-NL63 and HCoV-OC43 were amplified in the presence of different concentrations of brilacidin alone or combination of brilacidin and heparin. The intracellular viral level of amplified HCoV-OC43 was detected by immunofluorescence staining (**Figure 6A, 6B**), and the amplified HCoV-229E, HCoV-NL63 and HCoV-OC43 viruses released into culture medium were quantified by plaque assay (**Figure 6C, 6D, 6E**). Consistent with previous results, brilacidin dose-dependently inhibited replication of all three HCoVs (#1 vs #5 and #9). Addition of heparin dose-dependently decreased the inhibitory activity of brilacidin on replication of all three HCoVs (#5 vs #7 and #8; #9 vs #11 and #12).

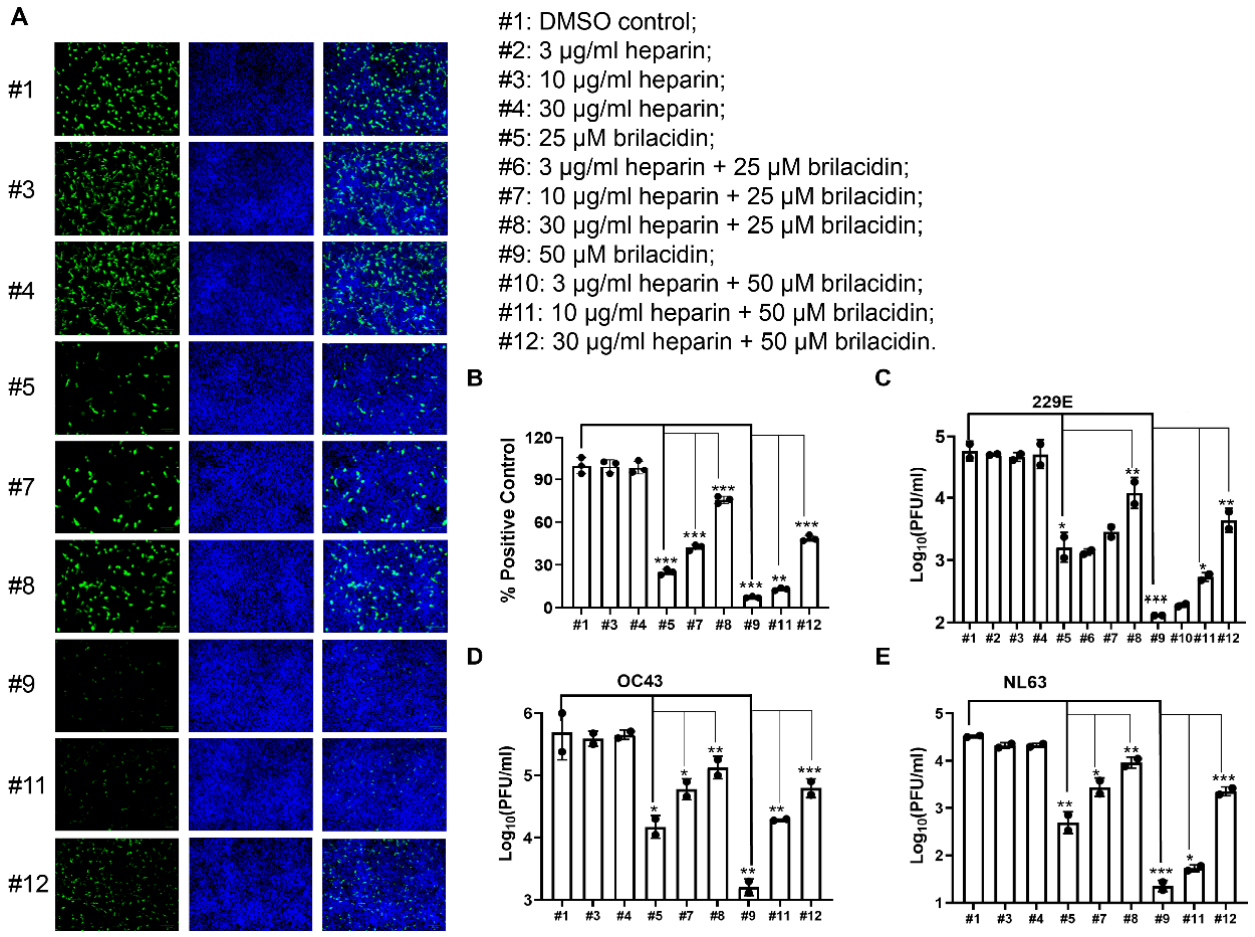

Figure 6. Heparin decreases the inhibitory activity of brilacidin on HCoVs replication in cell culture. RD cell, Huh-7 cell and Vero C1008 cell were infected with HCoV-OC43, HCoV-229E and HCoV-NL63 at an MOI of 0.1, respectively. Cell culture medium were collected 24 hpi to determine viral titers in each sample. RD cells were fixed 24 hpi for immunofluorescence staining, and intracellular HCoV-OC43 viral protein level was detected by HCoV-OC43 specific antibody. (A) Representative images of intracellular HCoV-OC43 viral protein level in RD cells detected by immunofluorescence staining; (B) Quantification of HCoV-OC43 viral protein level from panel A. Three groups (five for each group) of images were captured from three different areas in each sample, and fluorescent signals were quantified in Image J by calculating the percentage of viral

protein fluorescent signal (green) to nuclei fluorescent signal (blue) in pixels. Results shown are the average percentages from all three groups and normalized to DMSO control. Viral titers of viruses released into cell culture from each sample of (C) HCoV-OC43; (D) HCoV-229E; (E) HCoV-NL63. *, $p < 0.05$; **, $p < 0.01$; ***, $p < 0.001$ (student's *t*-test). All data are mean ± SD of two independent experiments.

Brilacidin has a strong synergistic antiviral effect with remdesivir in cell culture

Combination therapy is commonly used to slow down drug resistance development and reduce side effects [38, 39]. The antiviral effect of brilacidin and remdesivir in combination therapy was evaluated in HCoV-OC43 plaque assay using the combination indices method (**Figure 7**) [31]. Remdesivir, a SARS-CoV-2 polymerase inhibitor, is the only FDA-approved antiviral for treating COVID-19. Brilacidin and remdesivir were mixed at different ratios and the corresponding EC_{50} values for brilacidin and remdesivir were calculated. Combination indices (CIs) versus the EC_{50} values of brilacidin and remdesivir at different combination ratios were plotted (**Figure 7A**). The red line indicates additive effect; the right upper area above the red line indicates antagonism, while the left bottom area below the red line indicates synergy [37]. The CIs at all the combination ratios fell below the red line (**Figure 7A**), and the fractional inhibitory concentration index (**FICI**) which was used to determine synergistic effects of compounds are less than 0.5 at all combination ratios (**Figure 7B**), suggesting brilacidin has significant synergistic antiviral effect with remdesivir in the combination therapy.

A

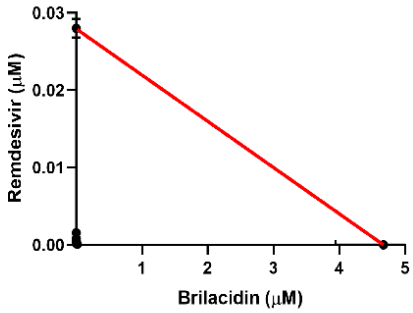

B

Combination ratio	EC_{50} in combination		EC_{50} alone		EC_{50} Equivalent		FICI
Brilacidin: Remdesivir	Brilacidin (μM)	Remdesivir (μM)	Brilacidin (μM)	Remdesivir (μM)	Brilacidin	Remdesivir	
4:1	0.01894	0.00007575			0.0039	0.0027	0.0066
2:1	0.002203	0.0001763			0.0005	0.0063	0.0068
1:1	0.001527	0.0002443			0.0003	0.0087	0.0090
1:2	0.001768	0.0005658	4.81 ± 0.95	0.028 ± 0.0012	0.0004	0.0202	0.0206
1:4	0.000656	0.0008396			0.0001	0.0300	0.0301
1:8	0.001212	0.001551			0.0003	0.0554	0.0556
1:16	0.002436	0.0007795			0.0005	0.0278	0.0283

Figure 7. Combination therapy of brilacidin with remdesivir in cell culture. (A) Plot of combination indices (CIs) versus the EC_{50} values of brilacidin and remdesivir at different combination ratios. (B) Table of combination therapy with EC_{50} and FICI values. EC_{50} equivalent was the ratio of EC_{50} of the compound in each combination to its EC_{50} alone. FICI was the sum of brilacidin and remdesivir EC_{50} equivalent in each combination. Data are mean ± SD of two independent experiments.

CONCLUSION

As the COVID19 pandemic keeps ongoing and variants continue to emerge, effective therapeutic interventions are urgently needed. Although three vaccines are currently available for prevention of COVID19, there is an urgent need for small molecular antivirals to help combat the pandemic. In this study, we investigated the antiviral activity and mechanism of action of brilacidin against multiple human coronaviruses. Our findings include: 1) Brilacidin has broad-spectrum antiviral activity

against HCoV-OC43, HCoV-NL63, and HCoV-229E viruses in cell culture; 2) Brilacidin inhibits SARS-CoV-2 pseudovirus entry into multiple cell lines, indicating that the inhibition is not cell type dependent; 3) Brilacidin has dual antiviral mechanisms of action which involves targeting both the virus and the host cell. Brilacidin has virucidal activity and blocks viral attachment to host cells by binding to HSPGs; 4) Brilacidin has strong synergistic antiviral effect with the FDA-approved SARS-CoV-2 antiviral remdesivir against HCoV-OC43 in cell culture.

The proposed antiviral mechanism of brilacidin is summarized in a model illustrated in **Figure 8**, which is supported by multiple lines of evidence. Our results showed that brilacidin has a dual antiviral mechanism against human coronaviruses including blocking viral attachment to host cells through binding to HSPGs and virucidal activity. HCoV-OC43, HCoV-NL63 and HCoV-229E showed dose-dependent decrease of replication in cells pretreated with brilacidin, and viral particles lose infectivity after incubation with brilacidin (**Figure 3**). Drug time-of-addition experiment suggested that brilacidin exerted its antiviral activity at two individual steps: viral attachment to host cell and early entry after entering into the host cells (**Figure 4**). The inhibition of viral attachment by brilacidin was confirmed in SARS-CoV-2 pseudovirus entry assay (**Figure 1**). DSF assay results demonstrated that brilacidin has no direct binding to SARS-CoV-2 spike protein RBD (**Table 1**). Competition experiment with heparin indicated that brilacidin binds to host cell surface HSPGs to block viral attachment to host cells. Addition of heparin dose-dependently decreased the inhibition of brilacidin in SARS-CoV-2 pseudovirus entry assay (**Figure 5**) and the replication of HCoV-OC43, HCoV-NL63 and HCoV-229E in cell culture (**Figure 6**).

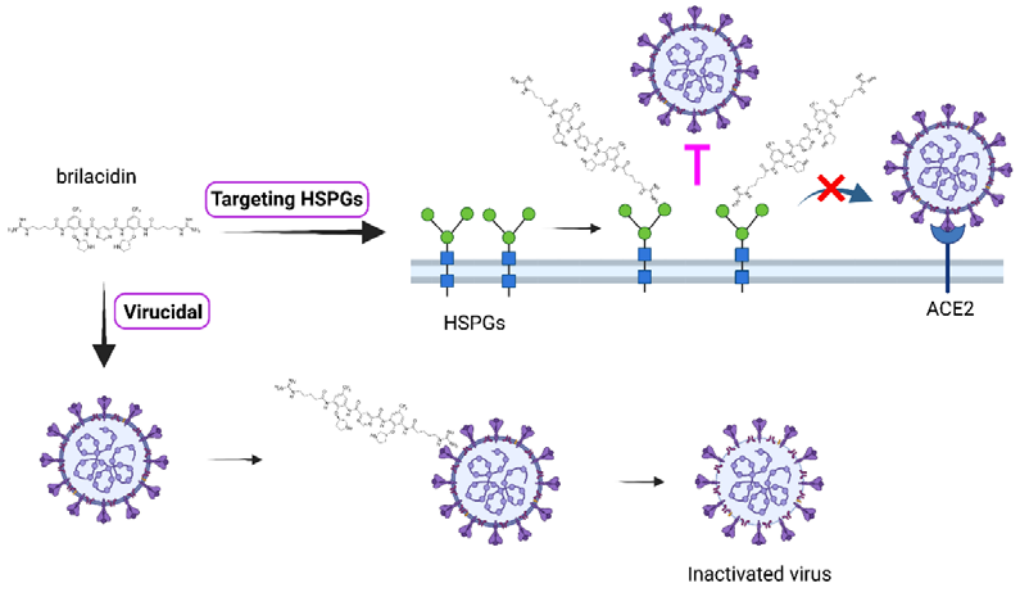

Figure 8. Proposed antiviral mechanism of brilacidin. Brilacidin has a dual antiviral mechanism including block viral attachment to host cells through binding to HSPGs and disrupt viral particles. The figure was created with BioRender.com.

In summary, our results indicate that brilacidin has a dual antiviral mechanism of action including targeting host cell surface HSPGs to block viral attachment and inactivating viral particles. This dual antiviral mechanism of action might slow down the pace of resistance development. Taken together, the broad-spectrum antiviral activity of brilacidin against coronaviruses warrants its further development as a broad-spectrum antiviral for the treatment of not only current COVID-19 but also future emerging coronaviruses.

METHORDS

Cell lines, viruses and reagents

Human rhabdomyosarcoma cell line (RD, ATCC® CCL-136™), African green monkey kidney cell line Vero C1008 (ATCC® CRL-1586™), Human hepatoma cell line Huh-7 (a kind gift from Dr. Tianyi Wang at University of Pittsburgh), and HEK293T expressing ACE2 (293T-ACE2, BEI Resources, NR-52511) cell lines were maintained in Dulbecco's modified eagle's medium (DMEM); Human fibroblast cell line MRC-5 (ATCC® CCL-171™), Human lung adenocarcinoma cell line Calu-3 (ATCC® HTB-55™), human Colorectal adenocarcinoma cell line (Caco-2, ATCC® HTB-37™) were maintained in eagle's minimum essential medium (EMEM, ATCC® 30-2003™). Both media were supplemented with 10% fetal bovine serum (FBS) and 1% penicillin-streptomycin antibiotics. Cells were kept at cell culture incubator (humidified, 5% CO_2/95% air, 37 °C). The following reagents were obtained through BEI Resources, NIAID, NIH: human coronavirus, HCoV-OC43, NR-52725; human coronavirus, HCoV-NL63, NR-470. HCoV-OC43 was propagated in RD cell line; HCoV-NL63 was initially propagated in 293T-ACE2 cell line and accommodated in Vero E6 cell line. HCoV-229E was obtained from Dr. Bart Tarbet (Utah State University) and amplified in Huh-7 or MRC-5 cell lines.

Antiviral assays

The antiviral activity of brilacidin was tested against HCoV-229E, HCoV-NL63 and HCoV-OC43 in Viral yield reduction (VYR) assays as previously described [30, 40-42]. Briefly, viruses were first replicated in the presence of serial concentrations of brilacidin (0, 0.39, 0.78, 1.56, 3.13, 6.25, 12.5, 25, 50, 100 µM). Progeny virions released in the supernatant were collected 24 hrs post-infection from each concentration of brilacidin

and the viral titers were determined by plaque reduction assay. Viruses were serially diluted 10 to 10^6 folds and infect the cells in 6-well plate. The infected cells were incubated at 33 or 37 °C for 1 h to allow virus adsorption. The viral inoculum was removed and an overlay containing 0.6% Avicel supplemented with 2% FBS in DMEM was added and incubated in the 33 or 37 °C incubator for 4 to 5 days. The plaque formation was detected by staining the cell monolayer with crystal violet. HCoV-229E and HCoV-OC43 plaque assays were carried out on RD cells and incubated at 33 °C, HCoV-NL63 plaque assay was performed on Vero C1008 cells and incubated at 37 °C. EC_{50} values were determined by plotting percentage of positive control versus $\log_{10}$ compound concentrations from best-fit dose response curves with variable slope in Prism 8.

Viral growth curves were obtained by replicating viruses in the presence or absence of 25 µM brilacidin at MOI of 0.1. Viruses in the supernatant were collected at the indicated time point post infection and viral titers were determined by plaque reduction assay as described in VYR assay section.

The antiviral activity of brilacidin tested in HCoV-OC43 plaque assay was carried out similarly as described in VYR assay, except that about 100 PFU of HCoV-OC43 virus was used to infect the cells in each well of 6-well plate and serial concentrations of brilacidin (0, 3.13, 6.25, 12.5, 25, 50, 100 µM) was included in the Avicel overlay. The plaque areas were quantified using Image J and the EC_{50} value was determined by plotting percentage of plaque area versus $\log_{10}$ compound concentrations from best-fit dose response curves with variable slope in Prism 8.

The antiviral activity of brilacidin against influenza and enterovirus D68 was carried out in plaque assay as previously described [36, 43, 44].

Cytotoxicity assay

Cytotoxicity of brilacidin was evaluated in different cell lines using the neutral red uptake assay as previously described [45, 46]. Cells were dispensed into 96-well plate at a density of 1×10^5 cells/ml at 100 µl/well. The growth medium was removed 18-24 hrs later and the cells were washed with 200 µl PBS supplemented with magnesium and calcium, and 200 µl fresh medium (+2% FBS) containing serial concentrations of brilacidin (0, 1.9, 3.9, 7.8, 15.6, 31.3, 62.5, 125 µM) was added into each well. After incubating at 37 °C incubator with 5% CO_2 for 48 hrs, cells were stained with 40 µg/ml neutral red for 2-4 hrs at 37 °C. The amount of neutral red uptaken by live cells was quantified by measuring the absorbance at 540 nm using a Multiskan FC Microplate Photometer (Fisher Scientific). The CC_{50} values were determined from best-fit dose response curves with variable slope in Prism 8.

Time of addition

Drug time-of-addition experiment was performed as previously described [30, 47]. Briefly, RD cells were seeded at 1×10^5 cells/well in 12-well plate with cover slip (Cat#: GG-12-1.5-PDL, Neuvitro) and infected with HCoV-OC43 at MOI of 1 and 25 µM brilacidin was added at different time points of viral life cycle as illustrated in Figure 3B. At 14 h post infection (hpi), cells were fixed with 4% formaldehyde for 10 min followed by permeabilization with 0.2% Triton X-100 for another 10 min. After blocking with 5% bovine serum, cells were sequentially stained with mouse anti-Coronavirus antibody, HCoV-OC43 strain, clone 541-8F (Cat#: MAB9012, Millipore Sigma, Burlington,

Massachusetts, USA) as primary antibody, and anti-mouse secondary antibody conjugated to Alexa-488 or Alexa546 (Cat # A-11029, Cat # A-11030, Thermo Scientific, Waltham, Massachusetts, USA). Nuclei were stained with 300 nM DAPI (Cat#: D1306, Thermo Scientific, Waltham, Massachusetts, USA) after secondary antibody incubation. For time of addition experiment using HCoV-OC43 and HCoV-229E in plaque assay, RD cells or Huh-7 cells were infected at MOI of 0.1 and 25 µM brilacidin was added at different time points of viral life cycle. Progeny virions released into the supernatant were harvested at 14 hpi and the viral titers were determined by plaque assay.

Pseudovirus assay

A pseudotype HIV-1-derived lentiviral particles bearing SARS-CoV-2 Spike and a lentiviral backbone plasmid encoding luciferase as reporter was produced in HEK293 T cells engineered to express the SARS-CoV-2 receptor ACE2 (293 T-ACE2 cells), as previously described [24]. The pseudovirus was then used to infect Vero C1008 cells, Huh-7 cells, Caco-2 cells, Calu-3 cells or 293 T-ACE2 cells in 96-well plates in the presence of serial concentrations of brilacidin (0, 3.13, 6.25, 12.5, 25, 50, 100 µM). Cells were lysed 48 hpi using the Bright-Glo Luciferase Assay System (Cat#: E2610, Promega, Madison, WI, USA), and the cell lysates were transferred to 96-well Costar flat-bottom luminometer plates. The relative luciferase units (RLUs) in each well were detected using Cytation 5 Cell Imaging Multi-Mode Reader (BioTek, Winooski, VT, USA). The IC_{50} values were determined from best-fit dose response curves with variable slope in Prism 8.

Differential scanning fluorimetry (DSF)

Direct binding of brilacidin with SARS-CoV-2 Spike protein receptor binding domain (RBD) was detected by differential scanning fluorimetry (DSF) using a Thermal Fisher QuantStudio 5 Real-Time PCR System as previously described [48, 49] with minor modifications. SARS-CoV-2 (2019-nCoV) Spike RBD-His Recombinant Protein (Cat. #: 40592-V08H, SinoBiological) was diluted in PBS buffer to a final concentration of 4 μM, and incubated with serial concentrations of brilacidin (25, 50, 100 μM) at 30 °C for 1 hr. DMSO was included as reference. 1× SYPRO orange (Thermal Fisher, Cat. #: S6650) was added and the fluorescence signal was recorded under a temperature gradient ranging from 20 to 95 °C (incremental step of 0.05 °C s^{-1}). The melting temperature (T_m) was calculated as mid log of the transition phase of the protein from the native to the denatured state using a Boltzmann model in Protein Thermal Shift Software v1.3. Δ T_m was calculated by subtracting melting temperature of protein in the presence of DMSO from the melting temperature of proteins in the presence of brilacidin.

Combination therapy

The combination antiviral effects of brilacidin and remdesivir were evaluated in HCoV-OC43 plaque assay in cell culture. Brilacidin was mixed with remdesivir at fixed EC_{50} ratios of 4:1, 2:1, 1:1, 1:2, 1:4, 1:8, and 1:16 separately. In each combination, nine 3-fold serial dilutions (equal to a 0.5 $\log_{10}$ unit decrease) of brilacidin and remdesiivr mixture were tested to plot the dose inhibition curve, based on which the EC_{50} values of individual brilacidin and remdesivir were determined in each combination. A combination indices (CIs) plot was used to depict the EC_{50} values of brilacidin and remdesivir at different combination ratios. The red line indicates the additive effect, and

above the red line indicates the antagonism, while below the red line indicates the synergy [50]. The fractional inhibitory concentration index (FICI) was calculated using the following formula: FICI = [(EC_{50} of brilacidin in combination)/(EC_{50} of brilacidin alone)] + [(EC_{50} of remdesivir in combination)/(EC_{50} of remdesivir alone)]. FICI <0.5 was interpreted as a significant synergistic antiviral effect [51].

AUTHOR INFORMATION

Corresponding Author

Jun Wang − Department of Pharmacology and Toxicology, College of Pharmacy, The University of Arizona, Tucson, Arizona 85721, United States; orcid.org/0000-0002-4845-4621; Phone: +1-520-626-1366; Email: junwang@pharmacy.arizona.edu

Authors

Yanmei Hu − Department of Pharmacology and Toxicology, College of Pharmacy, The University of Arizona, Tucson, Arizona 85721, United States

Hyunil Jo - Department of Pharmaceutical Chemistry, School of Pharmacy, University of California, San Francisco, California 94158, United States

William F. DeGrado - Department of Pharmaceutical Chemistry, School of Pharmacy, University of California, San Francisco, California 94158, United States

Author Contributions

J.W. and W.F.D. conceived and designed the study; Y.H. performed the pseudovirus neutralization assay, antiviral assays, time of addition experiment, immunofluorescence assays, thermal shift binding assay, and the combination therapy experiment. H. J. provided the brilacidin and acetyl brilacidin samples. Y.H. and J.W. wrote the manuscript.

Notes

The authors declare no competing financial interest(s).

ACKNOWLEDGMENTS

This research was partially supported by the National Institute of Allergy and Infectious Diseasess of Health (NIH) (grants AI147325, AI157046, and AI158775) and the Arizona Biomedical Research Commission Centre Young Investigator grant (ADHS18-198859) to J. W. Y.H. was supported by the NIH training grant T32 GM008804.

REFERENCES

1. Mesel-Lemoine, M., Millet, J., Vidalain, P. O., Law, H., Vabret, A., Lorin, V., Escriou, N., Albert, M. L., Nal, B., and Tangy, F. (2012) A human coronavirus responsible for the common cold massively kills dendritic cells but not monocytes, *J Virol 86*, 7577-7587.

2. Gagneur, A., Sizun, J., Vallet, S., Legr, M. C., Picard, B., and Talbot, P. J. (2002) Coronavirus-related nosocomial viral respiratory infections in a neonatal and paediatric intensive care unit: a prospective study, *J Hosp Infect 51*, 59-64.

3. Zumla, A., Hui, D. S., and Perlman, S. (2015) Middle East respiratory syndrome, *Lancet 386*, 995-1007.

4. Hui, D. S., E, I. A., Madani, T. A., Ntoumi, F., Kock, R., Dar, O., Ippolito, G., McHugh, T. D., Memish, Z. A., Drosten, C., Zumla, A., and Petersen, E. (2020) The continuing 2019-nCoV epidemic threat of novel coronaviruses to global health - The latest 2019 novel coronavirus outbreak in Wuhan, China, *Int J Infect Dis 91*, 264-266.

5. Center, C.-M.-J. H. C. R. (2021) https://coronavirus.jhu.edu/map.html

6. Collier, D. A., De Marco, A., Ferreira, I., Meng, B., Datir, R. P., Walls, A. C., Kemp, S. A., Bassi, J., Pinto, D., Silacci-Fregni, C., Bianchi, S., Tortorici, M. A., Bowen, J., Culap, K., Jaconi, S., Cameroni, E., Snell, G., Pizzuto, M. S., Pellanda, A. F., Garzoni, C., Riva, A., Collaboration, C.-N. B. C.-., Elmer, A., Kingston, N., Graves, B., McCoy, L. E., Smith, K. G. C., Bradley, J. R., Temperton, N., Ceron-Gutierrez, L., Barcenas-Morales, G., Consortium, C.-G. U., Harvey, W., Virgin, H. W., Lanzavecchia, A., Piccoli, L., Doffinger, R., Wills, M., Veesler, D., Corti, D., and Gupta, R. K. (2021) Sensitivity of SARS-CoV-2 B.1.1.7 to mRNA vaccine-elicited antibodies, *Nature 593*, 136-141.

7. Lopez Bernal, J., Andrews, N., Gower, C., Gallagher, E., Simmons, R., Thelwall, S., Stowe, J., Tessier, E., Groves, N., Dabrera, G., Myers, R., Campbell, C. N. J., Amirthalingam, G., Edmunds, M., Zambon, M., Brown, K. E., Hopkins, S., Chand,

M., and Ramsay, M. (2021) Effectiveness of Covid-19 Vaccines against the B.1.617.2 (Delta) Variant, *N Engl J Med 385*, 585-594.

8. Williams, T. C., and Burgers, W. A. (2021) SARS-CoV-2 evolution and vaccines: cause for concern?, *Lancet Respir Med 9*, 333-335.
9. Ageitos, J. M., Sanchez-Perez, A., Calo-Mata, P., and Villa, T. G. (2017) Antimicrobial peptides (AMPs): Ancient compounds that represent novel weapons in the fight against bacteria, *Biochem Pharmacol 133*, 117-138.
10. Magana, M., Pushpanathan, M., Santos, A. L., Leanse, L., Fernandez, M., Ioannidis, A., Giulianotti, M. A., Apidianakis, Y., Bradfute, S., Ferguson, A. L., Cherkasov, A., Seleem, M. N., Pinilla, C., de la Fuente-Nunez, C., Lazaridis, T., Dai, T., Houghten, R. A., Hancock, R. E. W., and Tegos, G. P. (2020) The value of antimicrobial peptides in the age of resistance, *Lancet Infect Dis 20*, e216-e230.
11. Ahmed, A., Siman-Tov, G., Hall, G., Bhalla, N., and Narayanan, A. (2019) Human Antimicrobial Peptides as Therapeutics for Viral Infections, *Viruses 11*.
12. Buda De Cesare, G., Cristy, S. A., Garsin, D. A., and Lorenz, M. C. (2020) Antimicrobial Peptides: a New Frontier in Antifungal Therapy, *mBio 11*.
13. Qin, Y., Qin, Z. D., Chen, J., Cai, C. G., Li, L., Feng, L. Y., Wang, Z., Duns, G. J., He, N. Y., Chen, Z. S., and Luo, X. F. (2019) From Antimicrobial to Anticancer Peptides: The Transformation of Peptides, *Recent Pat Anticancer Drug Discov 14*, 70-84.
14. Wang, G. (2020) The antimicrobial peptide database provides a platform for decoding the design principles of naturally occurring antimicrobial peptides, *Protein Sci 29*, 8-18.

15. Tytler, E. M., Anantharamaiah, G. M., Walker, D. E., Mishra, V. K., Palgunachari, M. N., and Segrest, J. P. (1995) Molecular basis for prokaryotic specificity of magainin-induced lysis, *Biochemistry 34*, 4393-4401.

16. Shai, Y. (1999) Mechanism of the binding, insertion and destabilization of phospholipid bilayer membranes by alpha-helical antimicrobial and cell non-selective membrane-lytic peptides, *Biochim Biophys Acta 1462*, 55-70.

17. Yeaman, M. R., and Yount, N. Y. (2003) Mechanisms of antimicrobial peptide action and resistance, *Pharmacol Rev 55*, 27-55.

18. Scott, R. W., and Tew, G. N. (2017) Mimics of Host Defense Proteins; Strategies for Translation to Therapeutic Applications, *Curr Top Med Chem 17*, 576-589.

19. Mensa, B., Howell, G. L., Scott, R., and DeGrado, W. F. (2014) Comparative mechanistic studies of brilacidin, daptomycin, and the antimicrobial peptide LL16, *Antimicrob Agents Chemother 58*, 5136-5145.

20. Kowalski, R. P., Romanowski, E. G., Yates, K. A., and Mah, F. S. (2016) An Independent Evaluation of a Novel Peptide Mimetic, Brilacidin (PMX30063), for Ocular Anti-infective, *J Ocul Pharmacol Ther 32*, 23-27.

21. Bakovic, A., Risner, K., Bhalla, N., Alem, F., Chang, T. L., Weston, W. K., Harness, J. A., and Narayanan, A. (2021) Brilacidin Demonstrates Inhibition of SARS-CoV-2 in Cell Culture, *Viruses 13*.

22. Zhang, Q., Chen, C. Z., Swaroop, M., Xu, M., Wang, L., Lee, J., Wang, A. Q., Pradhan, M., Hagen, N., Chen, L., Shen, M., Luo, Z., Xu, X., Xu, Y., Huang, W., Zheng, W., and Ye, Y. (2020) Heparan sulfate assists SARS-CoV-2 in cell entry and can be targeted by approved drugs in vitro, *Cell Discov 6*, 80.

23. Liu, L., Chopra, P., Li, X., Bouwman, K. M., Tompkins, S. M., Wolfert, M. A., de Vries, R. P., and Boons, G.-J. (2021) Heparan Sulfate Proteoglycans as Attachment Factor for SARS-CoV-2, *ACS Central Science 7*, 1009-1018.

24. Crawford, K. H. D., Eguia, R., Dingens, A. S., Loes, A. N., Malone, K. D., Wolf, C. R., Chu, H. Y., Tortorici, M. A., Veesler, D., Murphy, M., Pettie, D., King, N. P., Balazs, A. B., and Bloom, J. D. (2020) Protocol and Reagents for Pseudotyping Lentiviral Particles with SARS-CoV-2 Spike Protein for Neutralization Assays, *Viruses 12*.

25. Prabhakara, C., Godbole, R., Sil, P., Jahnavi, S., Gulzar, S. E., van Zanten, T. S., Sheth, D., Subhash, N., Chandra, A., Shivaraj, A., Panikulam, P., U, I., Nuthakki, V. K., Puthiyapurayil, T. P., Ahmed, R., Najar, A. H., Lingamallu, S. M., Das, S., Mahajan, B., Vemula, P., Bharate, S. B., Singh, P. P., Vishwakarma, R., Guha, A., Sundaramurthy, V., and Mayor, S. (2021) Strategies to target SARS-CoV-2 entry and infection using dual mechanisms of inhibition by acidification inhibitors, *PLoS Pathog 17*, e1009706.

26. Zhao, M., Su, P. Y., Castro, D. A., Tripler, T. N., Hu, Y., Cook, M., Ko, A. I., Farhadian, S. F., Israelow, B., Dela Cruz, C. S., Xiong, Y., Sutton, R. E., and Yale, I. R. T. (2021) Rapid, reliable, and reproducible cell fusion assay to quantify SARS-Cov-2 spike interaction with hACE2, *PLoS Pathog 17*, e1009683.

27. Shang, J., Wan, Y., Luo, C., Ye, G., Geng, Q., Auerbach, A., and Li, F. (2020) Cell entry mechanisms of SARS-CoV-2, *Proc. Natl. Acad. Sci. U. S. A. 117*, 11727-11734.

28. Tharappel, A. M., Samrat, S. K., Li, Z., and Li, H. (2020) Targeting Crucial Host Factors of SARS-CoV-2, *ACS Infect Dis 6*, 2844-2865.

29. Kong, Q., Xiang, Z., Wu, Y., Gu, Y., Guo, J., and Geng, F. (2020) Analysis of the susceptibility of lung cancer patients to SARS-CoV-2 infection, *Mol Cancer 19*, 80.

30. Smail, S. W., Saeed, M., Twana, A., Khudhur, Z. O., Younus, D. A., Rajab, M. F., Abdulahad, W. H., Hussain, H. I., Niaz, K., and Safdar, M. (2021) Inflammation, immunity and potential target therapy of SARS-COV-2: A total scale analysis review, *Food Chem Toxicol 150*, 112087.

31. Hu, Y., Meng, X., Zhang, F., Xiang, Y., and Wang, J. (2021) The in vitro antiviral activity of lactoferrin against common human coronaviruses and SARS-CoV-2 is mediated by targeting the heparan sulfate co-receptor, *Emerg Microbes Infect*, 1-32.

32. Tavassoly, O., Safavi, F., and Tavassoly, I. (2020) Heparin-binding Peptides as Novel Therapies to Stop SARS-CoV-2 Cellular Entry and Infection, *Mol Pharmacol 98*, 612-619.

33. Milewska, A., Zarebski, M., Nowak, P., Stozek, K., Potempa, J., and Pyrc, K. (2014) Human coronavirus NL63 utilizes heparan sulfate proteoglycans for attachment to target cells, *Journal of virology 88*, 13221-13230.

34. Naskalska, A., Dabrowska, A., Szczepanski, A., Milewska, A., Jasik, K. P., and Pyrc, K. (2019) Membrane Protein of Human Coronavirus NL63 Is Responsible for Interaction with the Adhesion Receptor, *Journal of virology 93*.

35. Kim, S. Y., Jin, W., Sood, A., Montgomery, D. W., Grant, O. C., Fuster, M. M., Fu, L., Dordick, J. S., Woods, R. J., Zhang, F., and Linhardt, R. J. (2020) Characterization of heparin and severe acute respiratory syndrome-related coronavirus 2 (SARS-CoV-2) spike glycoprotein binding interactions, *Antiviral Res 181*, 104873.

36. Ma, C., Hu, Y., Zhang, J., and Wang, J. (2020) Pharmacological Characterization of the Mechanism of Action of R523062, a Promising Antiviral for Enterovirus D68, *ACS Infect Dis 6*, 2260-2270.

37. Clausen, T. M., Sandoval, D. R., Spliid, C. B., Pihl, J., Perrett, H. R., Painter, C. D., Narayanan, A., Majowicz, S. A., Kwong, E. M., McVicar, R. N., Thacker, B. E., Glass, C. A., Yang, Z., Torres, J. L., Golden, G. J., Bartels, P. L., Porell, R. N., Garretson, A. F., Laubach, L., Feldman, J., Yin, X., Pu, Y., Hauser, B. M., Caradonna, T. M., Kellman, B. P., Martino, C., Gordts, P., Chanda, S. K., Schmidt, A. G., Godula, K., Leibel, S. L., Jose, J., Corbett, K. D., Ward, A. B., Carlin, A. F., and Esko, J. D. (2020) SARS-CoV-2 Infection Depends on Cellular Heparan Sulfate and ACE2, *Cell 183*, 1043-1057 e1015.

38. Bayat Mokhtari, R., Homayouni, T. S., Baluch, N., Morgatskaya, E., Kumar, S., Das, B., and Yeger, H. (2017) Combination therapy in combating cancer, *Oncotarget 8*, 38022-38043.

39. van der Pluijm, R. W., Tripura, R., Hoglund, R. M., Pyae Phyo, A., Lek, D., Ul Islam, A., Anvikar, A. R., Satpathi, P., Satpathi, S., Behera, P. K., Tripura, A., Baidya, S., Onyamboko, M., Chau, N. H., Sovann, Y., Suon, S., Sreng, S., Mao, S., Oun, S., Yen, S., Amaratunga, C., Chutasmit, K., Saelow, C., Runcharern, R.,

Kaewmok, W., Hoa, N. T., Thanh, N. V., Hanboonkunupakarn, B., Callery, J. J., Mohanty, A. K., Heaton, J., Thant, M., Gantait, K., Ghosh, T., Amato, R., Pearson, R. D., Jacob, C. G., Goncalves, S., Mukaka, M., Waithira, N., Woodrow, C. J., Grobusch, M. P., van Vugt, M., Fairhurst, R. M., Cheah, P. Y., Peto, T. J., von Seidlein, L., Dhorda, M., Maude, R. J., Winterberg, M., Thuy-Nhien, N. T., Kwiatkowski, D. P., Imwong, M., Jittamala, P., Lin, K., Hlaing, T. M., Chotivanich, K., Huy, R., Fanello, C., Ashley, E., Mayxay, M., Newton, P. N., Hien, T. T., Valecha, N., Smithuis, F., Pukrittayakamee, S., Faiz, A., Miotto, O., Tarning, J., Day, N. P. J., White, N. J., Dondorp, A. M., and Tracking Resistance to Artemisinin, C. (2020) Triple artemisinin-based combination therapies versus artemisinin-based combination therapies for uncomplicated Plasmodium falciparum malaria: a multicentre, open-label, randomised clinical trial, *Lancet 395*, 1345-1360.

40. Ma, C., Hu, Y., Townsend, J. A., Lagarias, P. I., Marty, M. T., Kolocouris, A., and Wang, J. (2020) Ebselen, Disulfiram, Carmofur, PX-12, Tideglusib, and Shikonin Are Nonspecific Promiscuous SARS-CoV-2 Main Protease Inhibitors, *ACS Pharmacol Transl Sci 3*, 1265-1277.

41. Hu, Y., Ma, C., Szeto, T., Hurst, B., Tarbet, B., and Wang, J. (2021) Boceprevir, Calpain Inhibitors II and XII, and GC-376 Have Broad-Spectrum Antiviral Activity against Coronaviruses, *ACS Infect Dis 7*, 586-597.

42. Xia, Z., Sacco, M., Hu, Y., Ma, C., Meng, X., Zhang, F., Szeto, T., Xiang, Y., Chen, Y., and Wang, J. (2021) Rational Design of Hybrid SARS-CoV-2 Main Protease Inhibitors Guided by the Superimposed Cocrystal Structures with the

Peptidomimetic Inhibitors GC-376, Telaprevir, and Boceprevir, *ACS Pharmacol Transl Sci 4*, 1408-1421.

43. Ma, C., Hu, Y., Zhang, J., Musharrafieh, R., and Wang, J. (2019) A Novel Capsid Binding Inhibitor Displays Potent Antiviral Activity against Enterovirus D68, *ACS Infect Dis 5*, 1952-1962.
44. Hu, Y., Kitamura, N., Musharrafieh, R., and Wang, J. (2021) Discovery of Potent and Broad-Spectrum Pyrazolopyridine-Containing Antivirals against Enteroviruses D68, A71, and Coxsackievirus B3 by Targeting the Viral 2C Protein, *J Med Chem 64*, 8755-8774.
45. Hu, Y., Zhang, J., Musharrafieh, R., Hau, R., Ma, C., and Wang, J. (2017) Chemical Genomics Approach Leads to the Identification of Hesperadin, an Aurora B Kinase Inhibitor, as a Broad-Spectrum Influenza Antiviral, *Int J Mol Sci 18*.
46. Hu, Y., Zhang, J., Musharrafieh, R. G., Ma, C., Hau, R., and Wang, J. (2017) Discovery of dapivirine, a nonnucleoside HIV-1 reverse transcriptase inhibitor, as a broad-spectrum antiviral against both influenza A and B viruses, *Antiviral Res 145*, 103-113.
47. Zhang, J., Hu, Y., Wu, N., and Wang, J. (2020) Discovery of Influenza Polymerase PA-PB1 Interaction Inhibitors Using an In Vitro Split-Luciferase Complementation-Based Assay, *ACS Chem Biol 15*, 74-82.
48. Ma, C., Sacco, M. D., Hurst, B., Townsend, J. A., Hu, Y., Szeto, T., Zhang, X., Tarbet, B., Marty, M. T., Chen, Y., and Wang, J. (2020) Boceprevir, GC-376, and calpain inhibitors II, XII inhibit SARS-CoV-2 viral replication by targeting the viral main protease, *Cell Res 30*, 678-692.

49. Musharrafieh, R., Kitamura, N., Hu, Y., and Wang, J. (2020) Development of broad-spectrum enterovirus antivirals based on quinoline scaffold, *Bioorg Chem 101*, 103981.

50. Abdelnabi, R., Geraets, J. A., Ma, Y., Mirabelli, C., Flatt, J. W., Domanska, A., Delang, L., Jochmans, D., Kumar, T. A., Jayaprakash, V., Sinha, B. N., Leyssen, P., Butcher, S. J., and Neyts, J. (2019) A novel druggable interprotomer pocket in the capsid of rhino- and enteroviruses, *PLoS Biol 17*, e3000281.

51. Odds, F. C. (2003) Synergy, antagonism, and what the chequerboard puts between them, *J Antimicrob Chemother 52*, 1.

For Table of Contents Use Only

Brilacidin, a COVID-19 Drug Candidate, demonstrates broad-spectrum antiviral activity against human coronaviruses OC43, 229E and NL63 through targeting both the virus and the host cell

Yanmei Hu[1], Hyunil Jo[2], William F. DeGrado[2], and Jun Wang[1]*

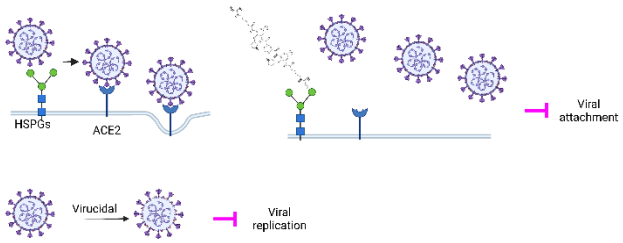

Brilacidin inhibits human coronaviruses through blocking viral attachment to HSPGs and inactivating the virus.